

# Effects of H-mode transition on plasma flow characteristics in the helical divertor of the Uragan-3M torsatron

CHECHKIN Viktor V., GRIGOR'EVA Lyudmila I., SOROKOVOY Yegor L.,  
 SOROKOVOY Eduard L., BELETSKII Aleksei A., SLAVNYJ Aleksandr S.,  
 LAVRENOVICH Jurij S., VOLKOV Yevgenij D., BURCHENKO Pavel Ya.,  
 TSYBENKO Sergej A., LOZIN Aleksei V., KULAGA Anatolij Ye.,  
 KURILO Dmitrij V., MIRONOV Jurij K., ROMANOV Vladislav S.

*Institute of Plasma Physics, National Science Center  
 "Kharkov Institute of Physics and Technology", Kharkov 61108, Ukraine*

In the  $l=3/m=9$  Uragan-3M (U-3M) torsatron with an open helical divertor and RF produced and heated plasmas, effects of H-mode transition on (i) diverted plasma flow (DPF) magnitude in the spacings between the helical coils and (ii) fast ion escape into DPF are studied by using arrays of plane Langmuir probes and electrostatic ion energy analyzers. Data have been obtained on how the amount and energy of lost ions change with transition in several field periods. A strong toroidal nonuniformity in ion loss has been observed. The island structure of the real U-3M magnetic configuration and the locality of RF power injection into the plasma are considered as possible reasons for such nonuniformity.

Key words: torsatron, divertor, H-mode, fast ions, ion loss, island structure

## 1. Introduction

In the Uragan-3M (U-3M) torsatron (Fig. 1,2) with an open natural helical divertor the plasma is RF produced and heated (multi-mode Alfvén resonance:  $\omega \lesssim \omega_{ci}(0)$ ). With this, a two-temperature ion energy distribution arises with a tail of suprathermal ions (Fig. 3) [1]. The faster ions (higher-temperature and suprathermal ones) can undergo the neoclassical transport  $1/v$ .

One more U-3M feature is a spontaneous transition to an H-like mode (Fig. 4) where an edge  $E_r \times B$  velocity shear occurs (or is enhanced), resulting in suppression of turbulence and turbulence-induced anomalous transport. It is supposed [2], that the fast ion orbit loss is responsible for  $E_r \times B$  shear formation [3]. Also, the specific for stellarators drift-orbit transport flux driven by helically trapped ions [4] can contribute to this process.

We study effects of H-transition on (i) diverted plasma flow (DPF) magnitude in the spacings between the helical coils and (ii) fast ion escape into DPF. Data have been obtained on how the amount and energy of lost ions change with transition in several field periods. A strong toroidal nonuniformity in ion loss has been observed. The island structure of the real U-3M magnetic configuration and the locality of RF power injection into the plasma are considered as possible reasons for such nonuniformity.

## 2. Experimental conditions

### Main parameters of U-3M:

$l = 3, m = 9, R = 1 \text{ m}; \bar{a} \approx 0.12 \text{ m}$

$1(\bar{a}) \approx 0.3; B_\phi = 0.72 \text{ T}$

$P_{RF} \lesssim 0.2 \text{ MW}, \bar{n}_e \sim 10^{18} \text{ m}^{-3}$

$T_e(0) \sim 500 \text{ eV}$

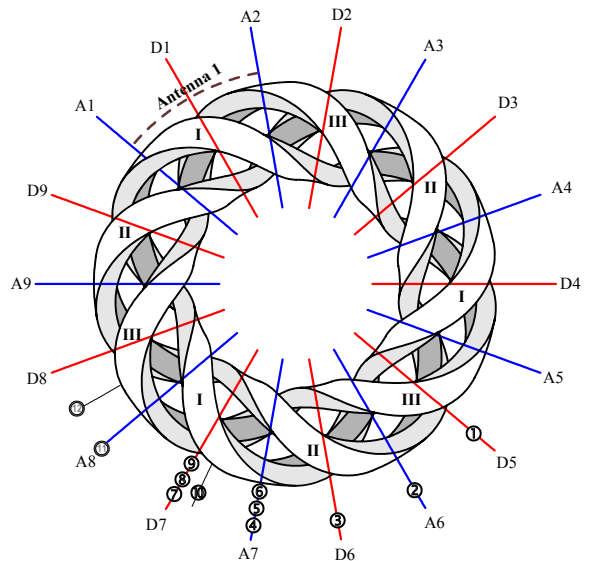


**Fig. 1.** Helical coils I, II, III; indicated are symmetric poloidal cross-sections A and D in all field periods I-9 (A1, D1, A2, D2,..., A9, D9).

1 – array of electrostatic ion energy analyzers (IEAs) in the top spacing D5 (D5 top)

2 – IEAs in A6 top

3 – IEAs in D6 top

4,5,6 – divertor electric probe arrays in A7 (see Fig. 2)

7,8,9 – divertor electric probe arrays in D7 (see Fig. 2)

10 – IEAs near D7 top

11 – IEAs in A8 top

12 – CXN energy analyzer detecting neutrals from the spacing between A8 top and D8 top

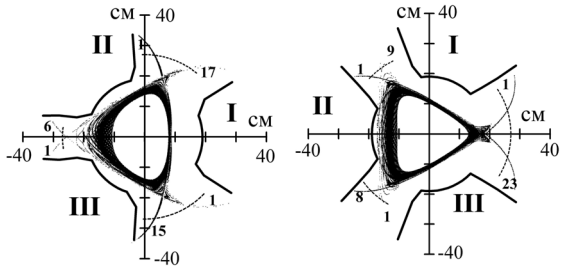


**Fig. 2.** Disposition of divertor electric probe arrays in the poloidal cross-sections A7 (left) and D7 (right).

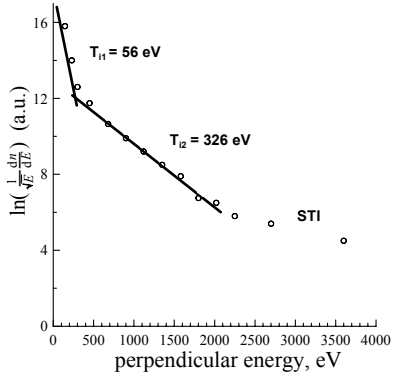


**Fig. 3.** CXN energy spectrum corresponds to two-temperature ion energy distribution + suprathermal tail.

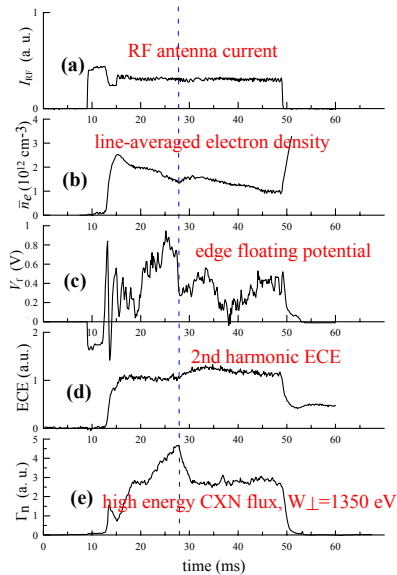


**Fig. 4.** Some indications of H-mode transition

### 3. H-mode-induced DPF changes (field period 7)

The H-transition results in substantial changes in the DPF magnitude estimated as maximum ion saturation current  $I_s$  in the corresponding spacing between the helical coils (Fig. 5).

In A7 (Fig. 5, left column)  $I_s$  decreases in all spacings while  $\bar{n}_e$  increases, evidencing a reduction of particle loss in this poloidal cross-section. The vertical DPF asymmetry decreases with transition: its degree is  $\alpha \approx 5$  before transition and drops to  $\alpha \approx 2$  after transition. This

means that the fast ion outflow is also reduced [5,6] as a part of the total particle loss reduction.

In D7 (Fig. 5, right column) DPF increases on the ion  $\nabla B$  drift side (top spacing, (b)) and outboard spacing over the midplane (d)), while it decreases in the bottom spacing (c) and in the outboard spacing under the midplane (e), i.e., on the electron drift side.

The DPF vertical asymmetry in D7 increases after the transition: from  $\alpha \approx 5$  to  $\alpha \approx 9$  for the top and bottom spacings and from  $\alpha \approx 3$  to  $\alpha \approx 4$  for the top and bottom legs in the outboard spacing. This indicates a rise of fast ion loss in this cross-section after the transition [5, 6].

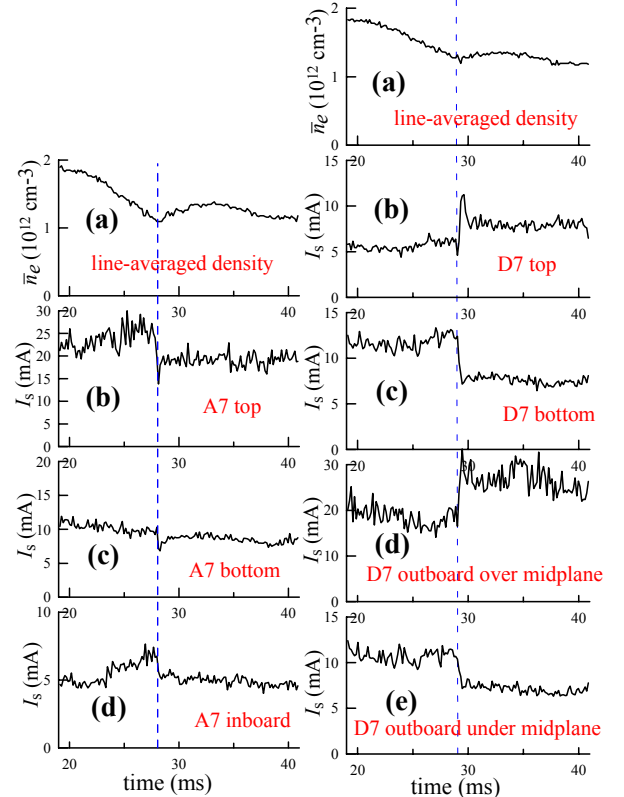


**Fig. 5.** H-transition-induced changes in DPF magnitude in cross-sections A7 (left column) and D7 (right column)

### 4 . Energies of ions outflowing to DPF

#### Cross-section A8, top spacing

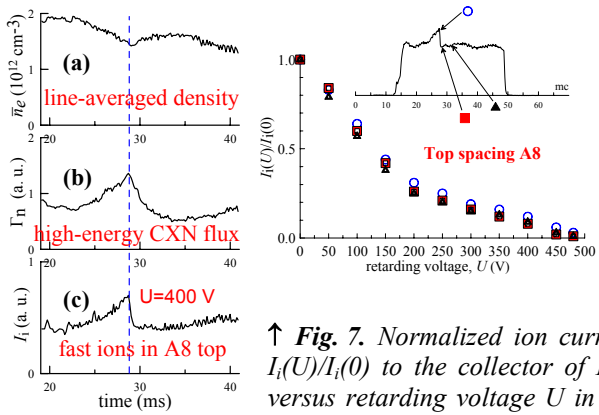
It follows from Fig. 6 that the fast ion loss roughly follows fast ion content in the confinement volume (represented by  $\Gamma_n$ ) and seems not to rise with transition.

The same is in A6 top.

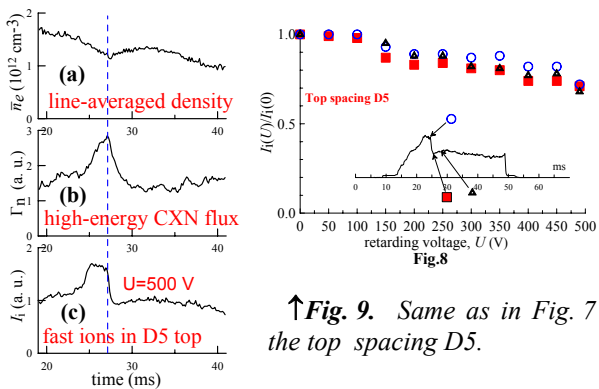
The energy of ions escaping to DPF on the ion  $\nabla B$  drift side in A8 top (Fig. 7) and A6 top do not change with transition and are minimum compared with D5 top, D6 top, D7 top (see below).

#### Cross-section D5, top spacing

Similar to A8 (and A6), the fast ion loss in D5 top roughly follows  $\Gamma_n$  and seems not to increase with transition (Fig. 8). The energies of ions escaping to DPF on the ion  $\nabla B$  drift side considerably exceed those in A8



↑ Fig. 6. Time evolution of density  $\bar{n}_e$  (a), high energy CXN flux  $\Gamma_n$  (b) and fast ion flow outflowing to DPF  $I_i$  (c) in the vicinity of H-transition in A8 top.

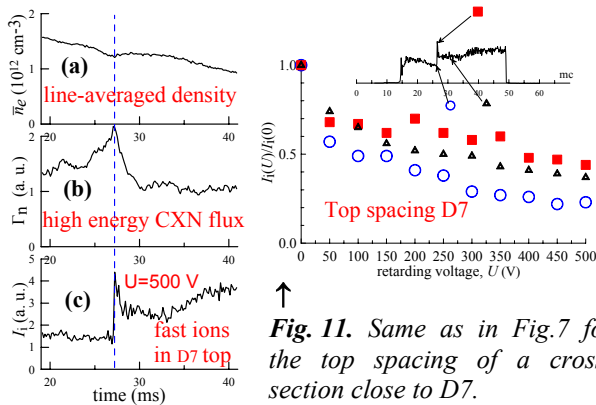


↑ Fig. 8. Same as in Fig. 6 for the top spacing D5

(and A6) but also do not change with transition (Fig.9).

The same is in the top spacing D6.

#### Top spacing in a cross-section close to D7 ( $\Delta\phi = 5^0$ )

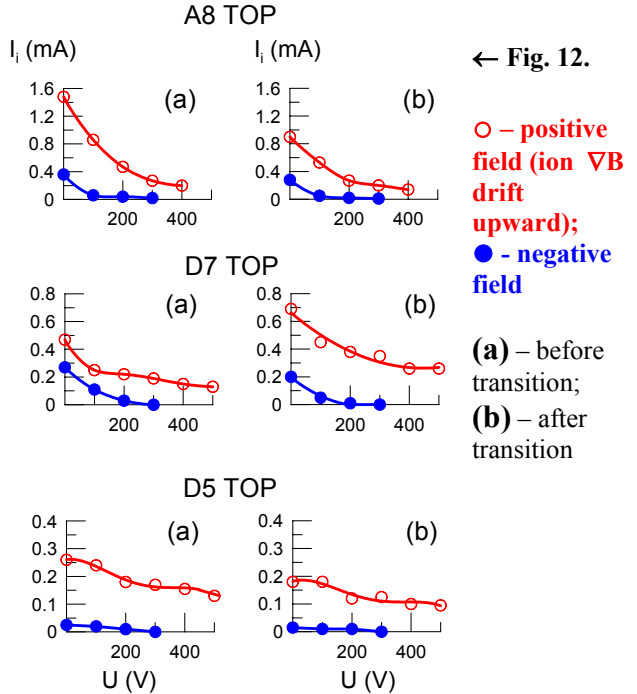


↑ Fig. 10. Same as in Fig. 6 for the top spacing of a cross-section close to D7.

Opposite to D5 top (Fig. 8) and D6 top, in the vicinity of D7 top the fast ion loss increases with transition (Fig. 10c) synchronously with a decrease of fast ion content in the confinement volume (Fig. 10b).

Also opposite to D5 top and D6 top, the energies of escaping ions on the ion  $\nabla B$  drift side increase with transition (Fig. 11).

#### Effects of magnetic field reversal



The  $I_i$  versus  $U$  plots measured at opposite directions of the magnetic field demonstrate that the fast ion loss dominates on the ion  $\nabla B$  drift side, being at least partially a real reason for the observed DPF vertical asymmetry in a heliotron/torsatron device like U-3M [5,6].

#### 6. Summaries and discussions

The DPF characteristics such as flow magnitude, its vertical asymmetry, energy of ions in DPF are distinct by a considerable toroidal nonuniformity both in the initial state (i.e., before transition) and by the character of changes induced by H-transition. Juxtaposing the data on time behavior of  $\bar{n}_e$ ,  $\Gamma_n$ , DPF magnitude (current  $I_s$ ) and current  $I_i$  of fast ions in DPF, we note the following.

1. In all spacings A7 the transition entails a DPF reduction. Taking the  $\bar{n}_e$  and ECE increase into account, this should be associated with a total particle loss reduction in the vicinity of A7. In a similar manner the fast ion component in DPF drops in A6 and A8 on the ion  $\nabla B$  drift side. At the same time, the fast ion content represented by  $\Gamma_n$  decreases in the confinement volume too. Therefore, strictly speaking, we can only presume that the transition does not result in a fast ion loss increase in the vicinity of A6 and A8.

The energies of ions outflowing to DPF in A6 and A8 do not change with transition. A valuable contribution of fast ion loss to DPF vertical asymmetry obviously follows from comparison of  $I_i(U)$  plots measured in the top spacings of A6 and A8 at opposite magnetic field directions.

**2.** Similar to A6 and A8: (i) the transition induces a DPF reduction in D5 and D6 on the ion  $\nabla B$  drift side. This is consistent with the  $\Gamma_n$  reduction and allows one to presume fast ion loss not to increase with transition; (ii) the energies of ions outflowing to DPF do not increase in D5 and D6, but they are considerably higher than in A6 and A8 both in the initial state and after the transition; (iii) the  $I_i(U)$  plots in the top spacings of D5 and D6 when measured at opposite directions of the magnetic field evidence a substantial contribution of fast ion loss to the DPF up-down asymmetry.

**3.** The H-transition-induced reduction of  $\Gamma_n$  indicates a rise of fast ion loss. Among all poloidal cross-sections having been explored, only in D7 on the ion drift side the H-transition-induced *increase* of DPF and of fast ion outflow occurs synchronously with the  $\Gamma_n$  *decrease*. Hence, toroidal segments can in principle arise in U-3M where fast ion loss increases with H-mode transition, this being one more manifestation of a strong toroidal non-uniformity of some plasma properties in U-3M.

The data available are not sufficient to clear up distinctly the factors responsible for the non-uniformities observed. Only some general considerations seem to be possible at present.

**1.** It has been observed experimentally [7] and confirmed numerically [8] that an island structure is inherent to the real magnetic configuration of the U-3M torsatron, that includes two main chains of magnetic islands at  $\iota = 1/4$ , each of them rotating poloidally when going round the torus and thus causing a difference between magnetic configurations in the same poloidal cross-sections belonging to different field periods. As is mentioned in [8], the real magnetic system of U-3M has actually only one field period instead of 9 ones in the ideal system, and we should not expect an exact reproducibility of all plasma characteristics from period to period.

**2.** Helically (locally!) trapped ions should be highly sensitive by their loss to the magnetic distortions in the field period where they are trapped. The  $1/v$  transport (effective ripple  $\epsilon_{\text{eff}}^{3/2}$ ) significantly increases near the islands [8]. Therefore an enhanced escape of fast ions into separate components of DPF is possible in principle (D5 top, D6 top).

**3.** In U-3M the ion orbit loss [3] and the drift-ion-orbit flux [4] are expected to be possible mechanisms driving the poloidal velocity  $E_r \times B$  to bifurcation with formation of gradients high enough to suppress the edge turbulence and turbulence-induced anomalous transport. The island-caused nonuniformity in fast ion loss distribution over the U-3M torus can presumably result in a nonuniformity in formation of edge plasma layers and in appearance of zones where the  $E_r$  profile is not favourable for fast ion confinement. Possibly, this could explain the occurrence of zones of enhanced fast ion loss after the transition (in particular, in the vicinity of D7 top).

**4.** The non-uniformity in toroidal distribution of some DPF characteristics could also originate from the local character of RF power injection into the U-3M plasma (RF antenna disposition in one field period only, RF

power injection through only one spacing between the helical coils, embracing of the plasma by the antenna only under one pair of the helical coils) and RF power deposition at the plasma edge. In these conditions we cannot exclude a nonuniformity in fast particle generation both along the torus and over the minor azimuth.

## References

- [1] E.D. Volkov *et al.*, Proc. 14th IAEA Conf. (Wurzburg 1992), Vol. 2, IAEA, Vienna, 679 (1993).
- [2] V.V. Chechkin *et al.*, Plasma Phys. Control. Fusion **48** A241 (2006).
- [3] K.S. Shaing, E.C. Crume, Phys. Rev. Lett. **63** 2369.
- [4] K.S. Shaing, Phys. Rev. Lett. **76** 4364 (1996).
- [5] V.V. Chechkin *et al.*, Nucl. Fusion **42** 192 (2002).
- [6] V.V. Chechkin *et al.*, Nucl. Fusion **43** 1175 (2003).
- [7] G.G. Lesnyakov *et al.*, Nucl. Fusion **32** 2157 (1992).
- [8] V.N. Kalyuzhnyj, V.V. Nemov, Fusion Science and Technology **46** 248 (2004).